

**CONFIDENTIAL**

Copy 220  
RM L55H26

NACA RM L55H26

7642



TECH LIBRARY KAFB, NM  
0144186

# RESEARCH MEMORANDUM

*Reg # 10348*

TRANSONIC WIND-TUNNEL INVESTIGATION OF THE EFFECTS OF  
INCIDENCE AND BODY INDENTATION ON THE WING LOADS  
OF A 45° SWEEPBACK WING-BODY COMBINATION

By Robert J. Platt, Jr.

Langley Aeronautical Laboratory  
Langley Field, Va.

**HADC  
TECHNICAL LIBRARY  
AFL 2811**

**NATIONAL ADVISORY COMMITTEE  
FOR AERONAUTICS**

WASHINGTON  
January 11, 1956

**CONFIDENTIAL**

Classification cancelled (or changed to UNCLASSIFIED)

By Authority of NASA Tech Pub Agreement #19  
(OFFICER AUTHORIZED TO CHANGE)

By 24 Aug 57

NAB  
GRADE OF OFFICER MAKING CHANGE)

31 Mar 61  
DATE



## NATIONAL ADVISORY COMMITTEE FOR AERONAUTICS

## RESEARCH MEMORANDUM

TRANSONIC WIND-TUNNEL INVESTIGATION OF THE EFFECTS OF  
INCIDENCE AND BODY INDENTATION ON THE WING LOADS  
OF A  $45^\circ$  SWEEPBACK WING-BODY COMBINATION

By Robert J. Platt, Jr.

## SUMMARY

The effects of an angle of incidence of  $4^\circ$  and body indentation on the wing loads of a sweptback wing-body combination have been investigated at Mach numbers from 0.6 to 1.2. The wing had an aspect ratio of 4, taper ratio of 0.3,  $45^\circ$  sweepback of the quarter-chord line, and NACA 65A006 airfoil sections parallel to the plane of symmetry.

At a constant wing angle of attack below the beginning of separation, the decrease in wing normal-force coefficient produced by incidence was nearly independent of Mach number and angle of attack. At a constant normal-force coefficient below the beginning of separation, the change in wing-panel bending-moment coefficient produced by incidence was slight and the change in wing pitching-moment coefficient was nearly independent of Mach number and normal-force coefficient.

The effects of body indentation on the wing loads at an incidence of  $4^\circ$  were to shift the center of pressure inboard and to delay the rearward movement of the center of pressure, which occurs at transonic speeds, to a higher Mach number.

## INTRODUCTION

A force-test investigation of a systematic series of wing-body configurations has been conducted in the Langley 8-foot transonic pressure tunnel to determine the effects of wing geometry and body indentation on the wing loads at transonic speeds. The first three phases of this investigation are reported in references 1 to 3. The fourth phase, reported herein, deals with the effects of incidence and body indentation on the wing loads of a sweptback wing-body combination. The data obtained with the wing at an angle of incidence are compared with data for the same

model at  $0^\circ$  incidence, reported in reference 1, to indicate the effects of incidence on wing loads.

The effects of wing incidence on the aerodynamic loads of a sweptback wing-body combination at transonic speeds have been previously investigated, by means of pressure measurements, for a somewhat different configuration than that of the present test, and are reported in reference 4. The present investigation provides additional data on the effect of incidence on wing loads at transonic speeds, obtained by means of a wing balance which measured only the forces and moments on the wing. The wing of the present investigation had an aspect ratio of 4, taper ratio of 0.3,  $45^\circ$  sweepback of the quarter-chord line, NACA 65A006 airfoil sections parallel to the plane of symmetry, and was mounted on the body at an incidence of  $4^\circ$ .

Body indentation has recently come into prominence as a means of reducing the drag rise at transonic speeds. In order to investigate the effects of body indentation on the wing loads, the wing was tested at an incidence of  $4^\circ$  with both a basic (unindented) body and with a body indented in accordance with the area-rule concept for  $M = 1.0$ .

The tests covered the Mach number range from 0.6 to 1.2 and an angle-of-attack range from  $0^\circ$  to  $20^\circ$  based on the wing-root chord line. The strain-gage balance measured the wing normal force, wing pitching moment, and the bending moment of each wing panel.

#### SYMBOLS

b	span of wing
$C_B$	bending-moment coefficient for wing panel, about fuselage center line, $\frac{4M_B}{qSb}$
$C_{m_W}$	pitching-moment coefficient for total wing in presence of body, about $0.25\bar{c}$ , $\frac{M_W}{qS\bar{c}}$
$C_{N_W}$	normal-force coefficient for total wing in presence of body, $\frac{N_W}{qS}$
c	section chord of wing measured parallel to plane of symmetry of model

$\bar{c}$	wing mean aerodynamic chord, $\frac{2}{S} \int_0^{b/2} c^2 dy$
$i$	wing incidence
$M$	free-stream Mach number
$M_B$	bending moment for wing panel about fuselage center line
$M_W$	pitching moment of wing in presence of body, about 0.25 $\bar{c}$
$N_W$	normal force on wing in presence of body
$q$	free-stream dynamic pressure, $\frac{\rho V^2}{2}$
$R$	Reynolds number, $\frac{\rho V \bar{c}}{\mu}$
$S$	total wing area (includes area covered by fuselage)
$V$	free-stream velocity
$\frac{x}{\bar{c}}$	longitudinal location of center of pressure in terms of mean aerodynamic chord, measured from leading edge of mean aerodynamic chord, $0.25 - \frac{C_{m_W}}{C_{N_W}}$
$\frac{y}{b/2}$	lateral location of center of pressure, in terms of wing semispan, measured from fuselage center line, $\frac{C_B}{C_{N_W}}$
$\alpha$	angle of attack of model based on wing-root chord line
$\mu$	coefficient of viscosity in free stream
$\rho$	mass density in free stream

## APPARATUS AND METHODS

## Tunnel

The test section of the Langley 8-foot transonic pressure tunnel is rectangular in cross section. The upper and lower walls of the tunnel are slotted to allow continuous operation through the transonic speed range. Some details of the test section are shown in figure 1. The sting support system shown in the figure was so designed that the model remained near the center line of the tunnel throughout the angle-of-attack range.

During the investigation the tunnel was operated at approximately atmospheric stagnation pressure and the stagnation temperature was automatically controlled and held constant at 120° F. The tunnel air was dried sufficiently to prevent condensation.

The tunnel was calibrated by means of an axial survey tube, provided with static-pressure orifices along its length, which extended from the entrance cone to the beginning of the diffuser. Some representative axial Mach number distributions at the center of the tunnel are shown in figure 2. The flow in the vicinity of the wing was satisfactorily uniform at all test Mach numbers. Local deviations from the average stream Mach number were no larger than 0.005 at subsonic speeds. With increases in Mach number above 1.0, these deviations increased but did not exceed 0.010 in the region of the wing at the highest test Mach number of 1.20.

## Models

The plan form of the wing tested and its dimensions are shown in figure 3. The wing had NACA 65A006 airfoil sections parallel to the plane of symmetry, an area of 1 square foot, an aspect ratio of 4, a taper ratio of 0.3, and 45° sweepback of the 25-percent chord line. The wing was constructed of steel.

The body frame was constructed of steel and contained a strain-gage balance designed to measure wing loads independently of any body load (figs. 3 and 4). The balance measured bending moment on each wing and normal force and pitching moment for both wings. The wing was mounted in the balance as shown in the detail of figure 3.

The coordinates of the basic (unindented) body and the body indented for  $M = 1.0$  are given in table I. Between stations 22.5 and 36.9 the body contour was formed by an outer shell. A gap of about 0.030 inch was left between the wing and the outer body shell to prevent fouling of the wing on the body. For tests with the basic body, the gap was sealed

with soft rubber tubing as shown in the detail of figure 3. For tests with the indented body, however, the thinness of the outer shell did not permit the gap to be sealed.

A photograph of the model with the basic body is shown in figure 5.

The angle of attack was measured by a strain-gage attitude transmitter mounted in the body frame ahead of the wing.

#### Tests

The angle of attack, based on the wing-root chord line, extended from  $0^\circ$  to  $20^\circ$  unless limited by the maximum allowable load on the strain-gage balance. The Mach number range extended from 0.60 to 1.20. However, data were not recorded in the Mach number range between 1.03 and 1.12 because in this range the data may have been affected by reflections of the fuselage bow wave from the tunnel walls. The variation of Reynolds number (based on a mean aerodynamic chord of 6.580 in.) with Mach number is shown in figure 6.

#### Accuracy

The addition of the rubber seals in the gap between the wing and body shell was found to decrease the strain-gage-balance sensitivity as much as 5 percent. For this reason, separate balance calibrations were used for the configuration with seals (basic body) and the configuration without seals (indented body).

The accuracy of the strain-gage measurements is estimated to be as follows:

M	Accuracy of -		
	$C_{N_W}$	$C_{m_W}$	$C_B$
0.6	$\pm 0.009$	$\pm 0.004$	$\pm 0.008$
1.2	$\pm 0.004$	$\pm 0.002$	$\pm 0.004$

The average stream Mach number was held within  $\pm 0.003$  of the nominal value given in the figures.

The error associated with the strain-gage attitude transmitter, used to measure the angle of attack, is estimated to be  $\pm 0.1^\circ$ . However, an additional error in angle of attack arose from the deflection of the balance produced by the pitching moment. The effect of the maximum pitching moment reached was to decrease the wing angle of attack nearly  $0.2^\circ$ , which occurred at supersonic speeds at the highest test angles of attack. No correction for this effect has been made to the data.

As previously mentioned, the wing-indented-body configuration was tested with an unsealed gap between the wing and body. Some idea of the effect of this gap can be obtained from reference 1 wherein the wing of the present investigation, at  $0^\circ$  incidence, was tested in the presence of the basic body with both a sealed and unsealed gap. The differences obtained with and without the seal were generally within the estimated accuracy of the measurements at angles of attack below where pitch-up tendencies were indicated. From this, it is believed that the effect of the gap on the data of the present investigation is slight at angles of attack below the break in the pitching-moment curve.

During the present test a cathetometer, sighted on the wing tip, was used to measure the twist of the wing under load. The maximum twist was about  $-0.8^\circ$  and occurred at the highest Mach numbers. No corrections to the data for aeroelastic effects have been made.

## RESULTS AND DISCUSSION

### Effect of Incidence

Wing normal force.— The effect of wing incidence on the aerodynamic load carried by a wing is basically a problem of body interference. If the wing of a wing-body combination is at a fixed angle of attack and the body angle of attack is varied, any resulting change in the load on the wing is induced by the varying body angle of attack. For the present configuration, the change in wing normal force produced by an angle of incidence of  $4^\circ$  may be seen in figures 7(a) and 8(a) for the wing with the basic and indented bodies, respectively. The data for an angle of incidence of  $0^\circ$  are reproduced from reference 1 for comparison with the data for the same models at an incidence of  $4^\circ$  obtained in the present investigation. A decrease in normal force is produced by the incidence as shown by comparison of the two sets of data. Since only the force on the wing was measured, and the angle of attack is based on the wing-root chord line, the increment in normal force at a constant angle of attack is induced by the change in the body upwash.

Figures 7(a) and 8(a) indicate that the increment in wing normal force is very nearly constant with increasing angle of attack until



separation begins, as evidenced by a decrease in the slope of the normal-force curve. At somewhat higher angles of attack the increment tends to decrease, but this effect is not pronounced, probably because separation begins at the wing tip, which is less influenced by a change in the body upwash than are sections near the wing root. However, when stall is reached the effect of incidence appears to be negligible.

Figures 7(a) and 8(a) also show that the change in normal force on the wing resulting from incidence is but little affected by Mach number up to the highest test Mach number of 1.20.

Wing pitching moment.- Figure 7(b) shows the variation of wing pitching-moment coefficient with wing normal-force coefficient for the wing in the presence of the basic body. Shown for comparison are the data for the same model at an angle of incidence of  $0^\circ$ , taken from reference 1. In figure 8(b) is a similar comparison of pitching-moment data for the wing in the presence of the indented body. The effect of incidence is, in general, to produce a more negative pitching-moment coefficient. This may be explained by the fact that the smaller body upflow for the incidence case tends to reduce the load carried by the inboard sections of the wing at a given normal-force coefficient. Because the wing is swept back, this gives rise to a more negative pitching moment.

Figures 7(b) and 8(b) show that the negative increment in pitching-moment coefficient, which results from wing incidence, is very nearly constant with increasing wing normal-force coefficient until separation begins. The beginning of separation is indicated by a tendency for the wing to pitch up, which occurs on this wing at a normal-force coefficient of about 0.4 at the lower Mach numbers. After separation begins, the increment in pitching moment produced by the incidence is no longer nearly constant and even becomes positive at some normal-force coefficients.

The data indicate little or no effect of Mach number on the pitching-moment increment produced by incidence, up to the highest test Mach number of 1.20. In figure 8(b) there appears to be some decrease in pitching-moment increment at the two highest test Mach numbers, but this should be discounted because the data for the model without incidence do not pass through the origin.

Bending-moment coefficient.- The effect of  $4^\circ$  incidence on the wing panel bending moment is shown in figures 7(c) and 8(c) for the wing with the basic body and the indented body, respectively. For the incidence case, test points are shown for both the left-wing panel bending moment and the right-wing bending moment. Data from reference 1 for  $0^\circ$  incidence are shown for comparison.

The effect of incidence on the bending moment at a constant wing normal-force coefficient, although small, is to increase the bending

moment. Incidence, therefore, moves the center of pressure outboard on the wing panel.

Comparison with reference 4. - Reference 4 reports an investigation of the effects of an angle of incidence of  $4^\circ$  on the wing loads of a somewhat different sweptback wing-body combination than that of the present investigation. In comparison, the model of reference 4 had a larger taper ratio, the wing was twisted, and the body was smaller than that used in the present test. Data were obtained through the transonic range by means of pressure measurements.

The effects of incidence on the wing loads of the present model, previously discussed, are generally similar to those found in reference 4 except for a small effect on the wing-panel bending moment which was not evident in the data of reference 4. However, the changes in normal-force and pitching-moment coefficient produced by incidence tend to be more constant in the present test than in the investigation of reference 4. For instance, in reference 4, the increment in normal-force coefficient tended to decrease with angle of attack, whereas in the present test the increment is very nearly constant until separation begins. These small differences between the results of the two investigations may be due both to the difficulty of measurement and to the differences in the models.

#### Effect of Body Indentation

The lateral and longitudinal locations of the center of pressure have been computed from the previously presented faired curves of wing-panel bending-moment coefficient and wing pitching-moment coefficient as a function of wing normal-force coefficient. These results, shown in figure 9, give the center-of-pressure position as a function of Mach number for the wing at an incidence of  $4^\circ$  in the presence of the basic and indented bodies. The figure therefore indicates the effect of indentation on the center-of-pressure location. The longitudinal position of the center of pressure is but little affected by body indentation except that the rearward movement, which occurs at transonic speeds, is delayed by the body indentation. At normal force coefficients above 0.4, this effect disappears, which may possibly be due to the lack of a seal at the wing-body juncture in the case of the indented body. The spanwise center of pressure is generally moved inboard from 1 percent to  $2\frac{1}{2}$  percent of the semispan by the indentation. A spanwise shift of this order would be expected from the additional wing area exposed by the indentation.

The preceding effects of indentation on the center-of-pressure location do not completely agree with the data of reference 1, which gives

a comparison of the center of pressure for the same wing and bodies as the present investigation but at  $0^\circ$  angle of incidence. The data of reference 1 indicate that little or no change in the lateral center-of-pressure location is produced by body indentation at supersonic Mach numbers and low normal-force coefficients.

#### CONCLUDING REMARKS

An investigation of the effects of an angle of incidence of  $4^\circ$  on the wing loads of a  $45^\circ$  sweptback wing in the presence of a basic and an indented body has been made at transonic speeds. At a constant wing angle of attack below the beginning of separation, the decrease in wing normal-force coefficient produced by incidence was nearly independent of Mach number and angle of attack. At a constant normal-force coefficient below the beginning of separation, the change in wing-panel bending-moment coefficient produced by incidence was slight and the change in wing pitching-moment coefficient was nearly independent of Mach number and normal-force coefficient. Therefore, it appears that a good estimate of the effect of incidence on wing loads at transonic speeds can be easily made for other configurations if the effect of incidence is known at low speeds, either from tests or calculations.

The effects of body indentation on the wing loads at an incidence of  $4^\circ$  were to shift the center of pressure inboard and to delay the rearward movement of the center of pressure, which occurs at transonic speeds, to a higher Mach number.

Langley Aeronautical Laboratory,  
National Advisory Committee for Aeronautics,  
Langley Field, Va., August 19, 1955.

## REFERENCES

1. Delano, James B., and Mugler, John P., Jr.: Transonic Wind-Tunnel Investigation of the Effects of Taper Ratio and Body Indentation on the Aerodynamic Loading Characteristics of a  $45^\circ$  Sweptback Wing in the Presence of a Body. NACA RM L54L28, 1955.
2. Platt, Robert J., Jr., and Brooks, Joseph D.: Transonic Wind-Tunnel Investigation of the Effects of Sweepback and Thickness Ratio on the Wing Loads of a Wing-Body Combination of Aspect Ratio 4 and Taper Ratio 0.6. NACA RM L54L31b, 1955.
3. Mugler, John P., Jr.: Transonic Wind-Tunnel Investigation of the Aerodynamic Loading Characteristics of a  $60^\circ$  Delta Wing in the Presence of a Body With and Without Indentation. NACA RM L55G11, 1955.
4. Robinson, Harold L.: The Effects of Wing Incidence on the Aerodynamic Loading Characteristics of a Sweptback Wing-Body Combination at Transonic Speeds. NACA RM L54G23b, 1954.

TABLE I  
BODY COORDINATES

Forebody		Afterbody			
Station, in. from nose	Radius, in.	Basic body		Indented body	
		Station, in. from nose	Radius, in.	Station, in. from nose	Radius, in.
0	0	22.500	1.875	22.500	1.875
.225	.104	26.500	1.875	23.380	1.875
.5625	.193	27.692	1.868	23.692	1.863
1.125	.325	28.692	1.862	24.692	1.819
2.250	.542	29.692	1.849	25.692	1.749
3.375	.726	30.692	1.825	26.692	1.662
4.500	.887	31.692	1.789	27.692	1.579
6.750	1.167	32.692	1.745	28.692	1.505
9.000	1.390	33.692	1.694	29.692	1.468
11.250	1.559	34.692	1.638	30.692	1.469
13.500	1.683	35.692	1.570	31.692	1.490
15.750	1.770	36.692	1.486	32.692	1.505
18.000	1.828	36.900	1.468	33.692	1.506
20.250	1.864	37.500	1.408	34.692	1.502
		38.500	1.298	35.692	1.491
		39.500	1.167	36.692	1.471
		40.500	1.030	36.900	1.468
		41.250	.937	36.900 to 41.250	*

\* Same as basic body.

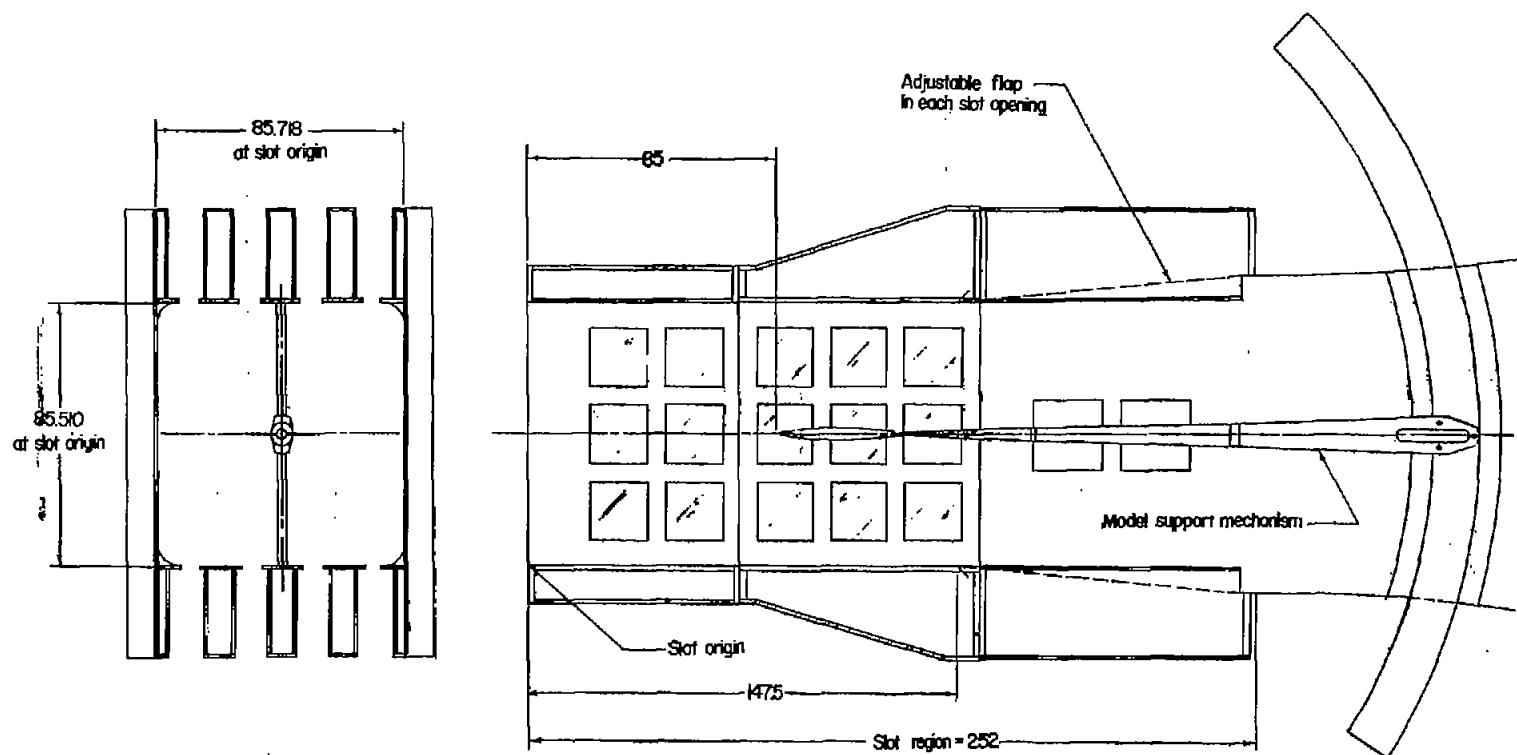


Figure 1.- Details of test section and location of model in the Langley 8-foot transonic pressure tunnel. All dimensions are in inches.

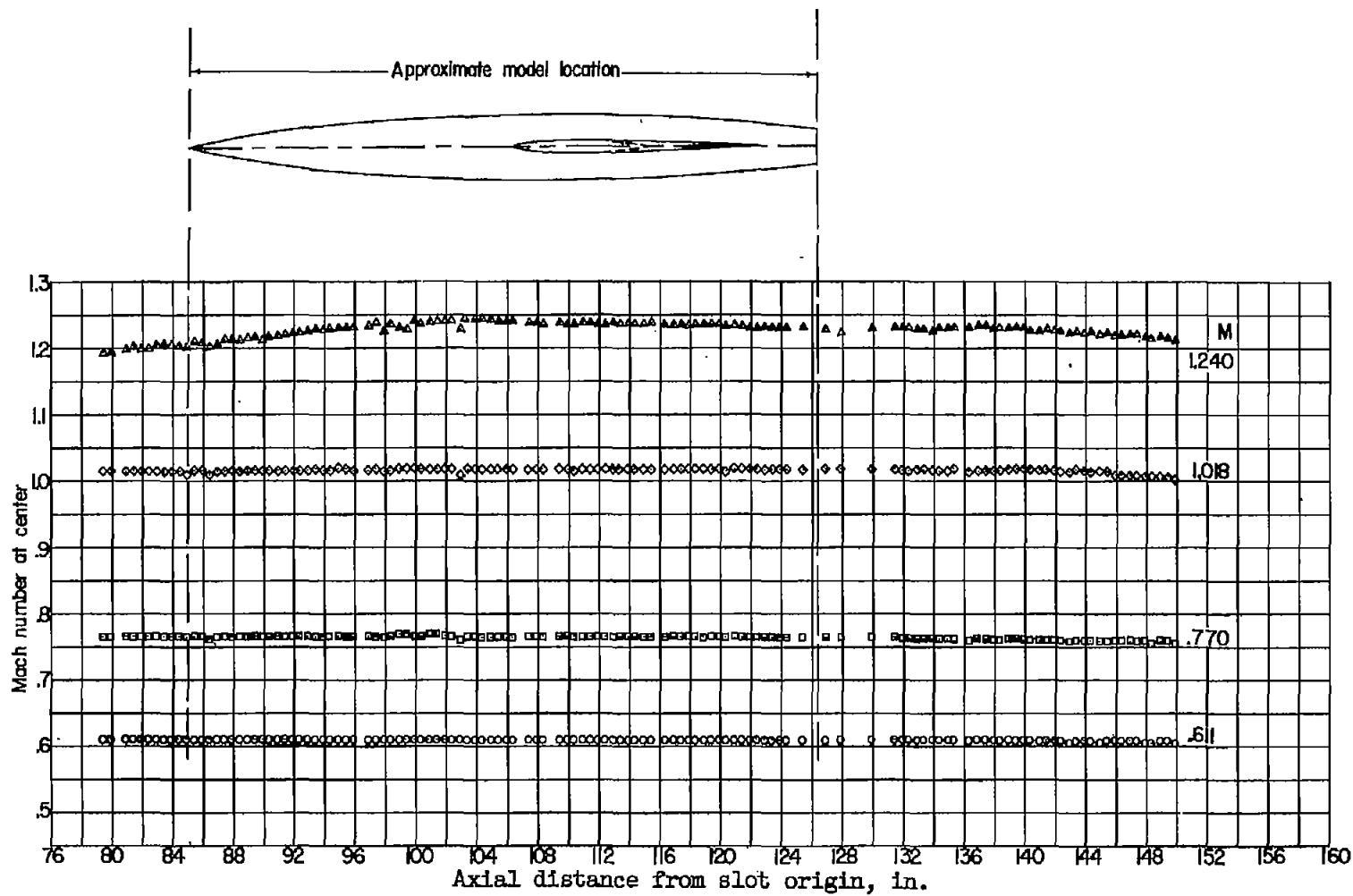
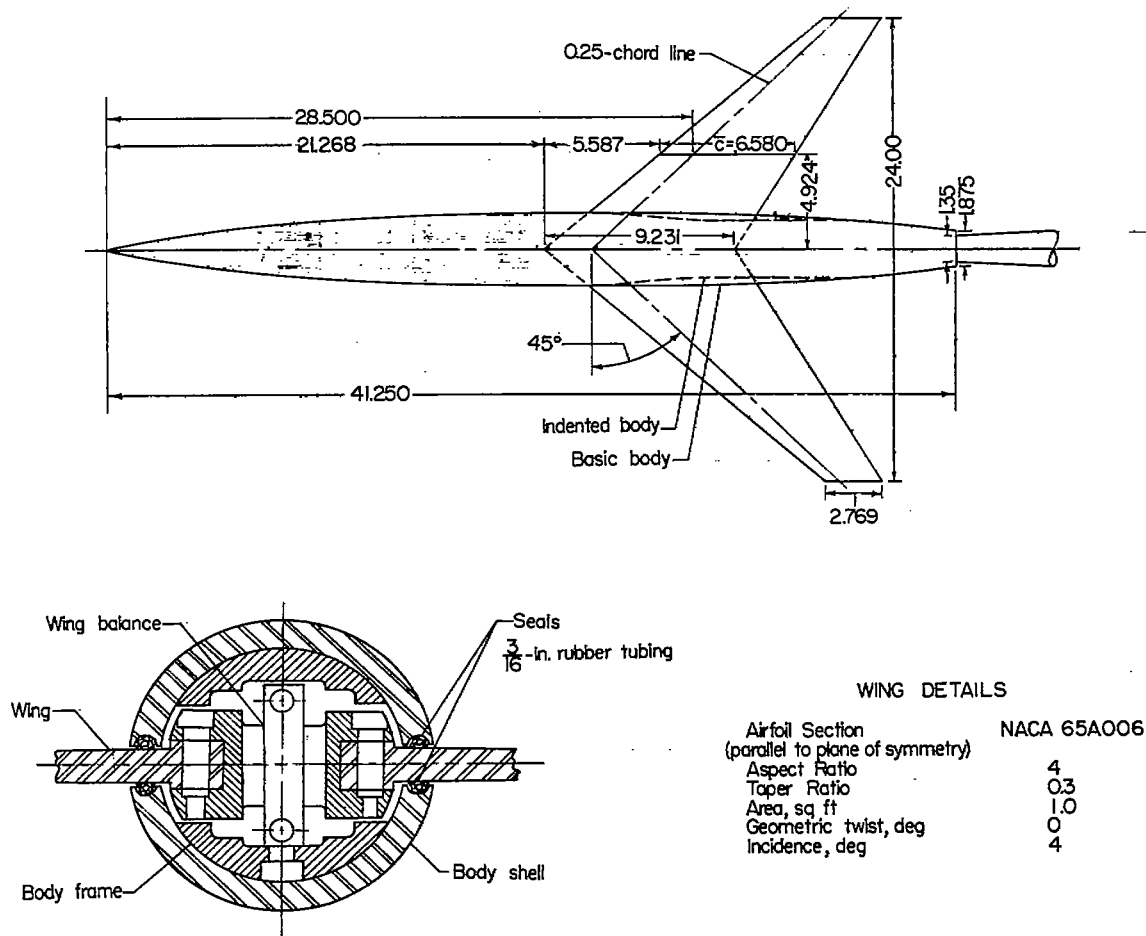


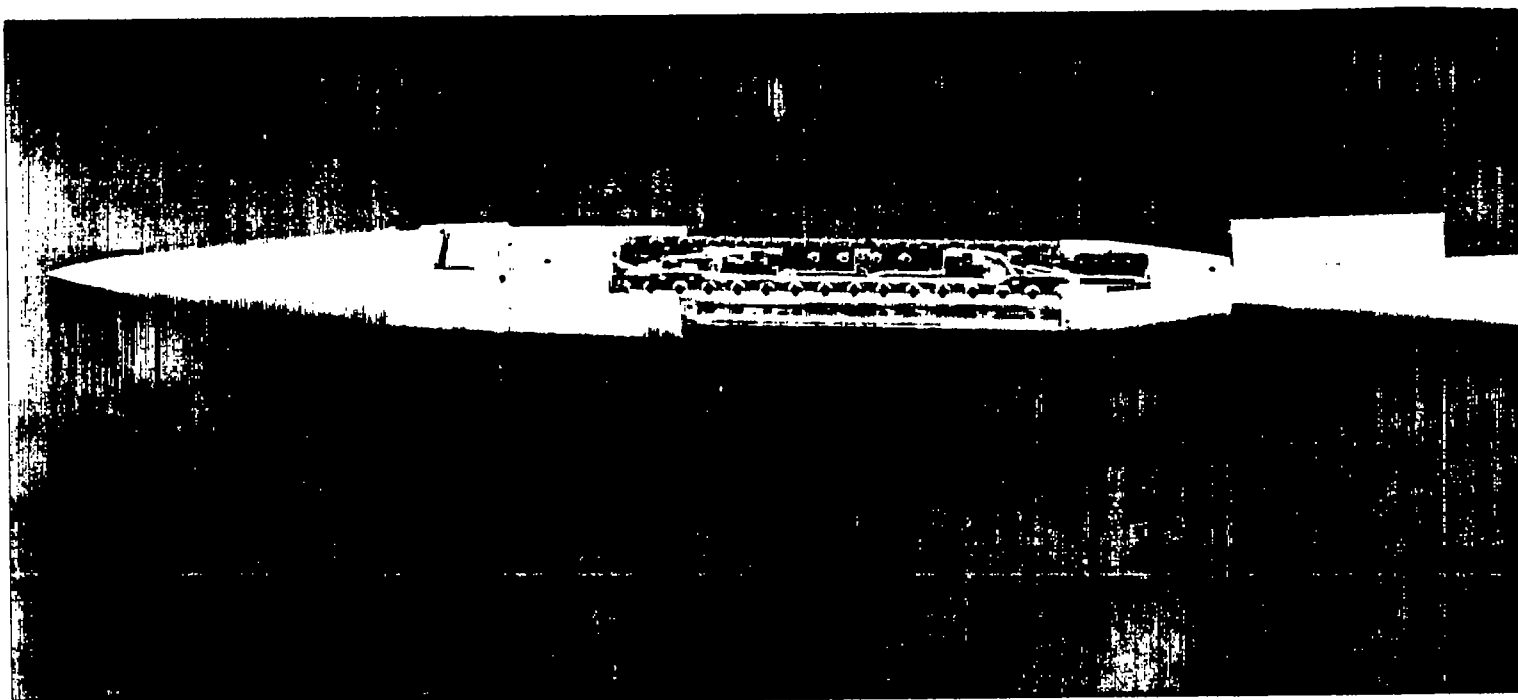
Figure 2.- Typical Mach number distributions in the test section of the Langley 8-foot transonic pressure tunnel during this investigation.



Section showing details of wing balance and seals

Figure 3.- Wing-body configurations tested. All dimensions are in inches except as noted.





L-84806

Figure 4.- Strain-gage balance mounted in the body.

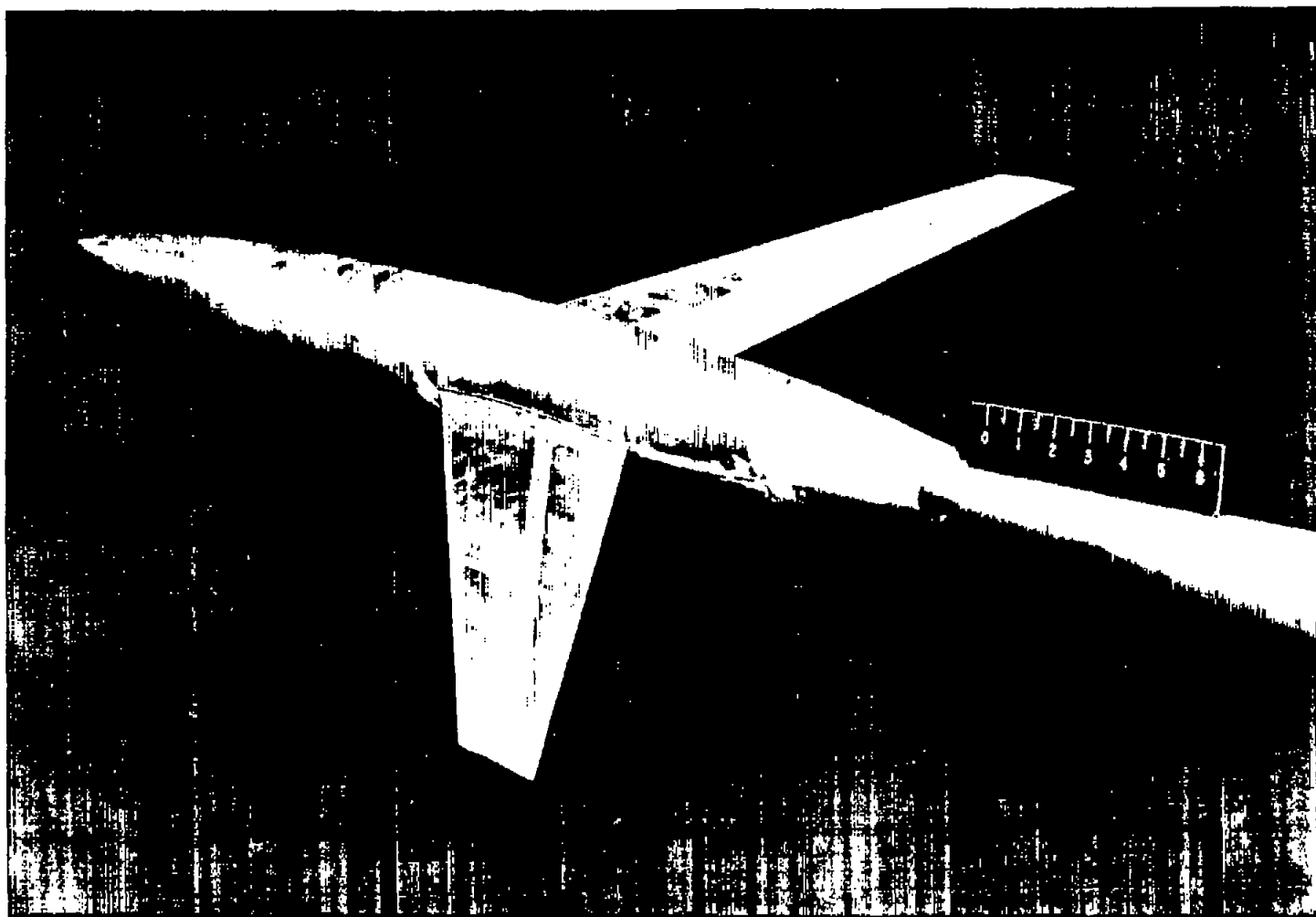


Figure 5.- Model with basic body. Wing incidence  $0^\circ$ .

L-84819

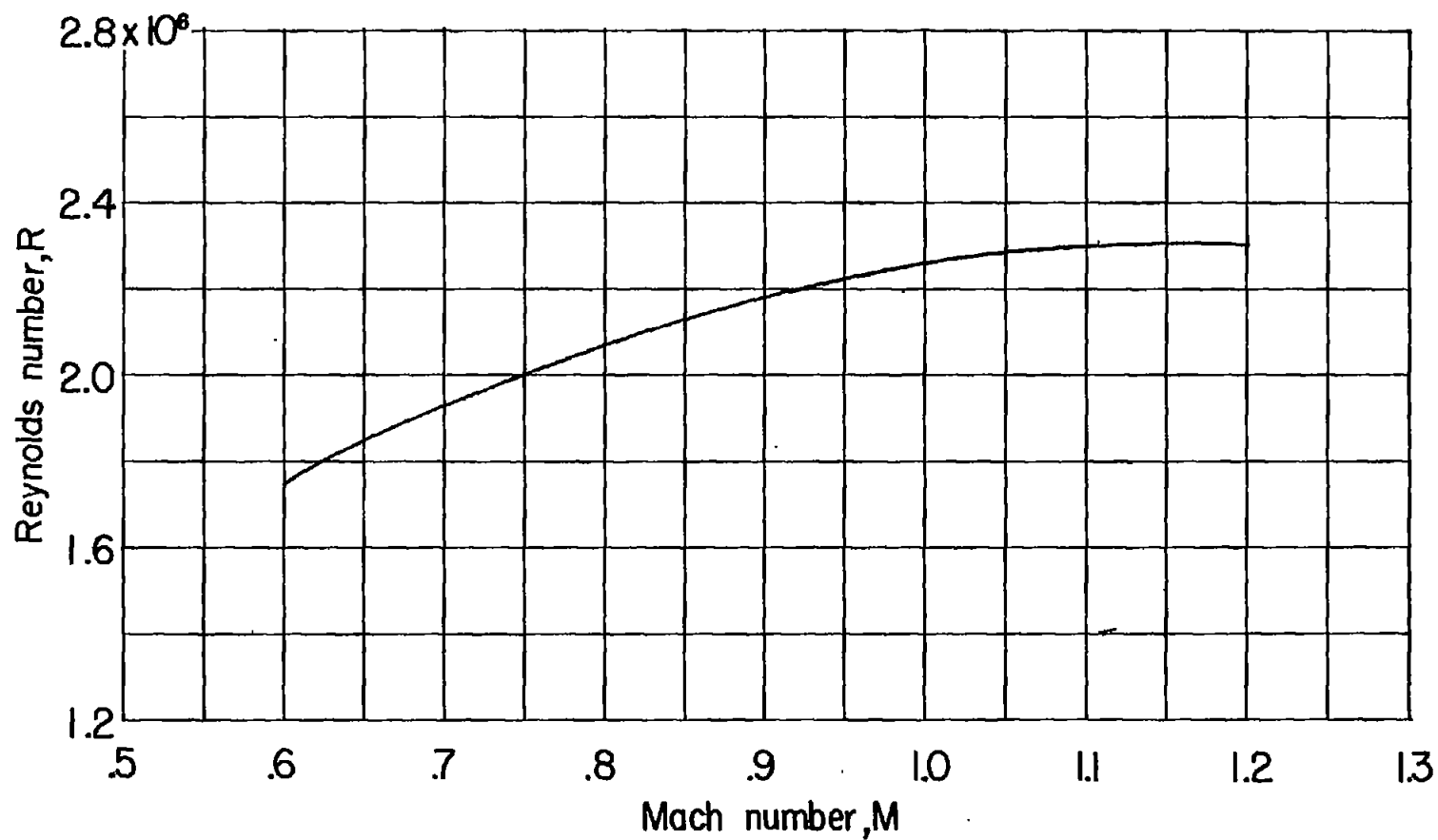
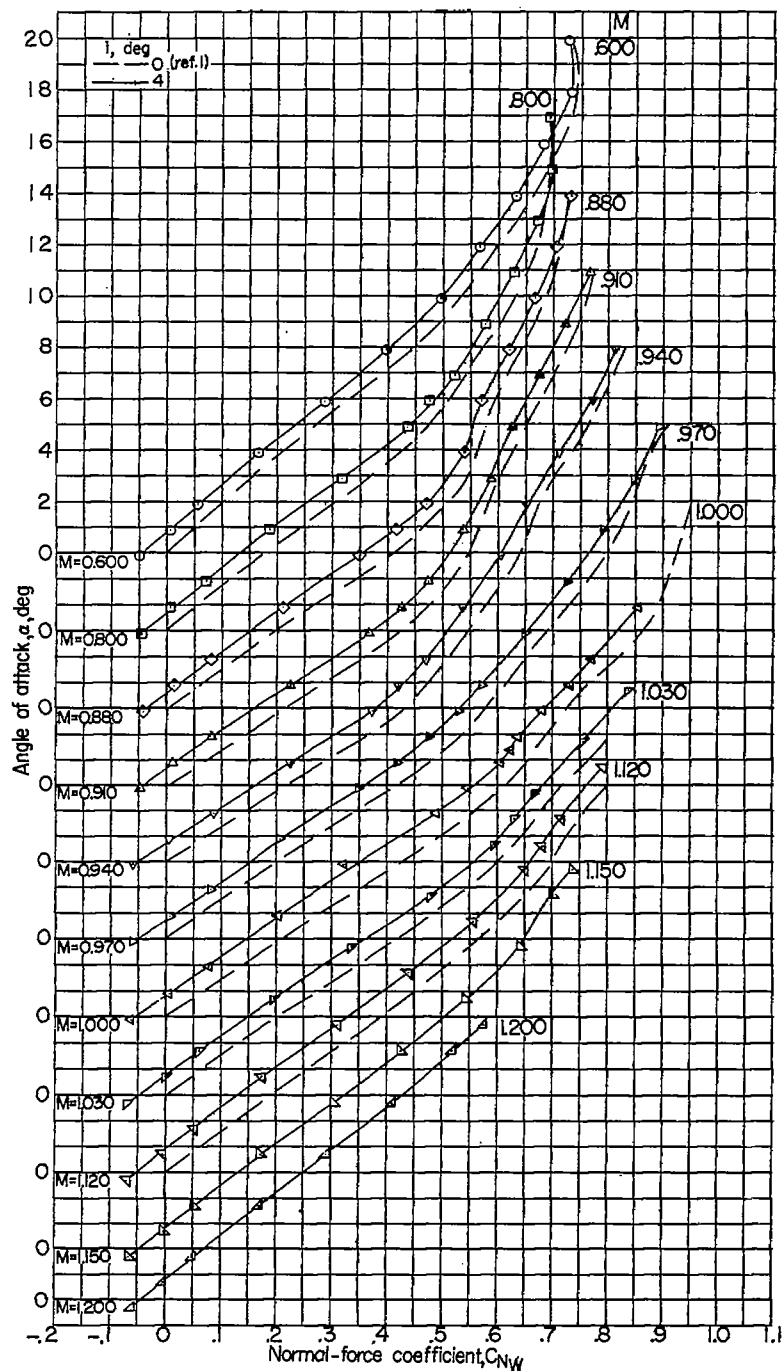


Figure 6.- Variation of Reynolds number with Mach number.



(a) Variation of  $\alpha$  with  $C_{N_W}$ .

Figure 7.- Aerodynamic characteristics of the wing of a wing-body combination. Basic body; wing incidence  $4^\circ$  and  $0^\circ$ .

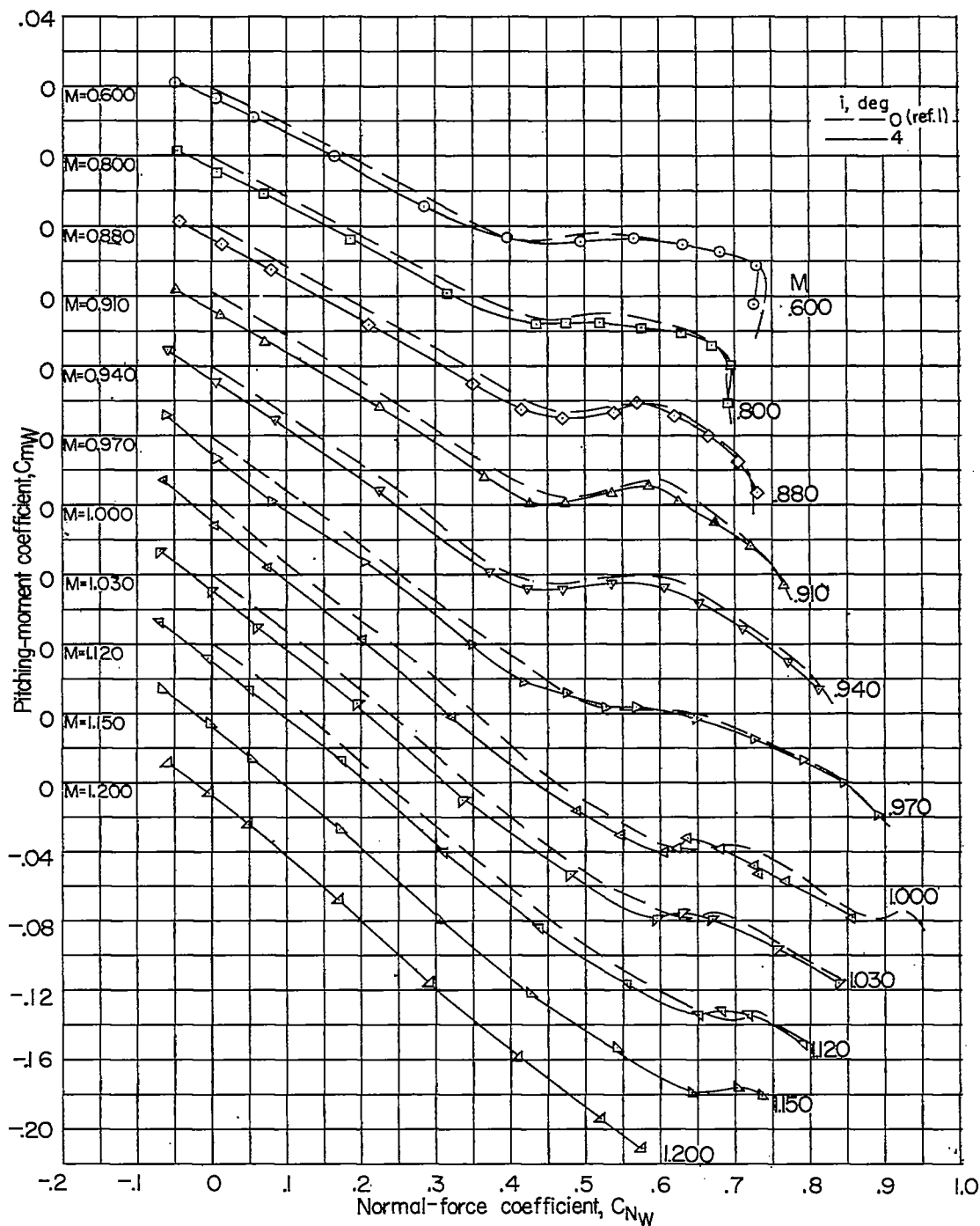
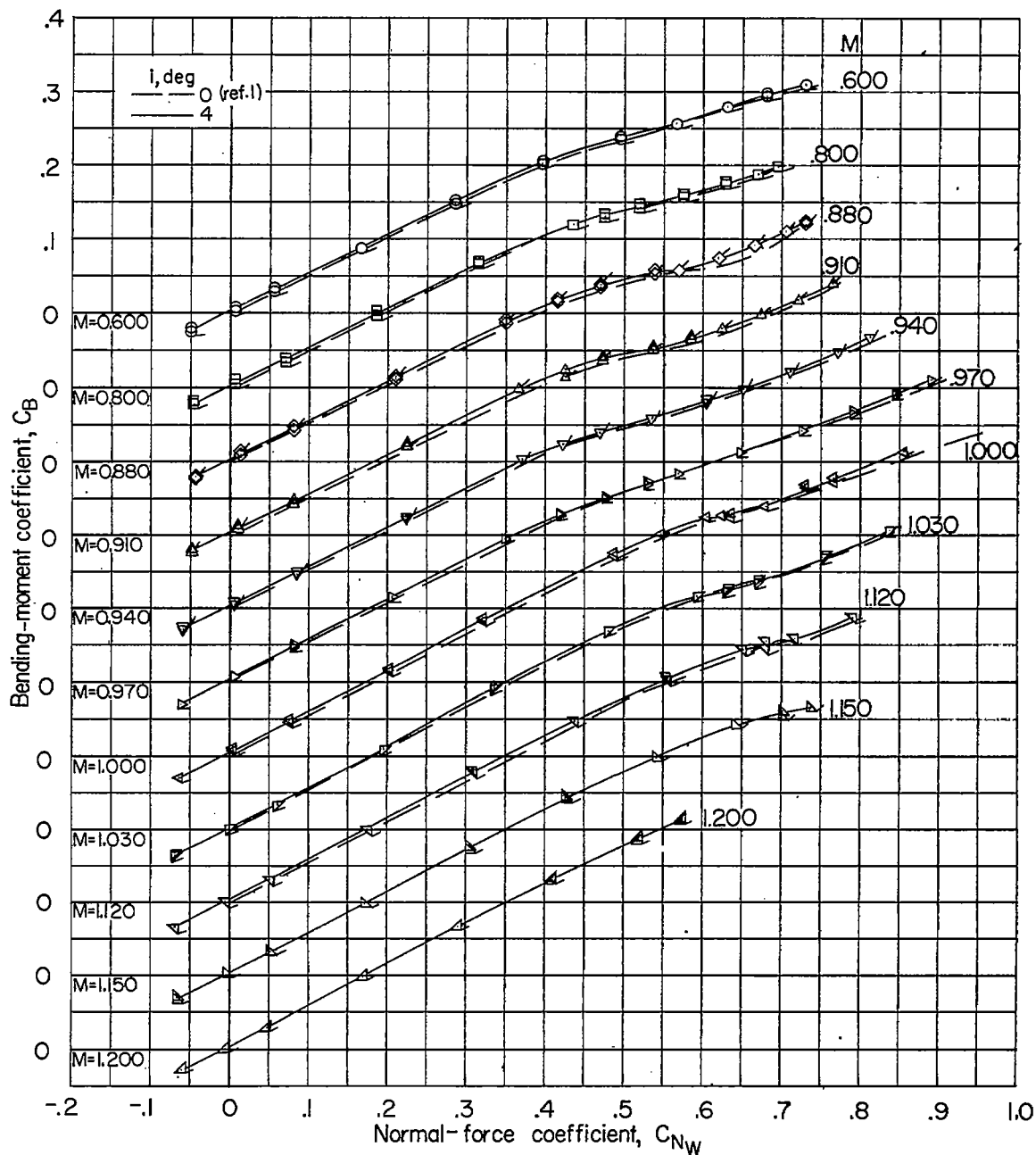
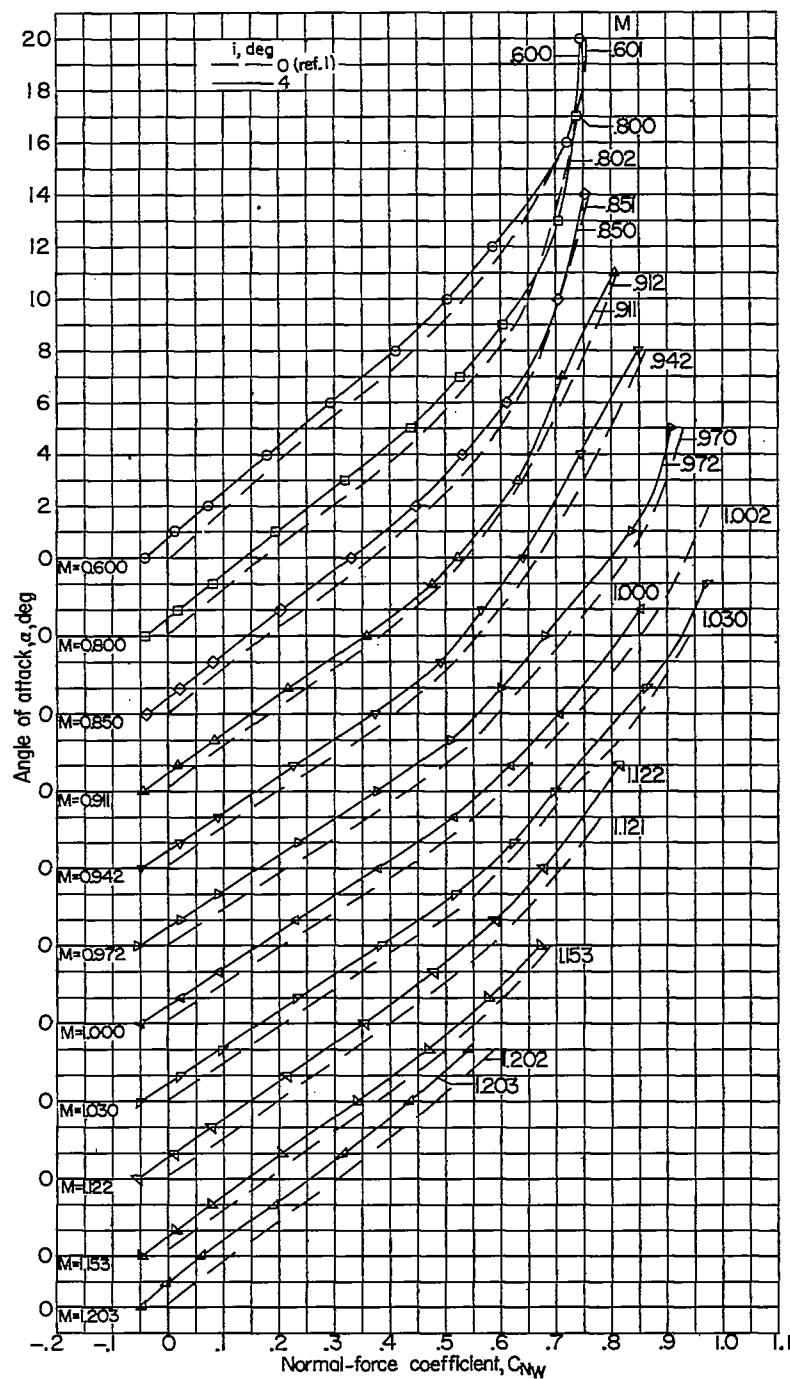
(b) Variation of  $C_{mW}$  with  $C_{Nw}$ .

Figure 7.- Continued.



(c) Variation of  $C_B$  with  $C_{NW}$  for right- and left-wing panels. Flagged symbols indicate left-wing panel.

Figure 7.- Concluded.



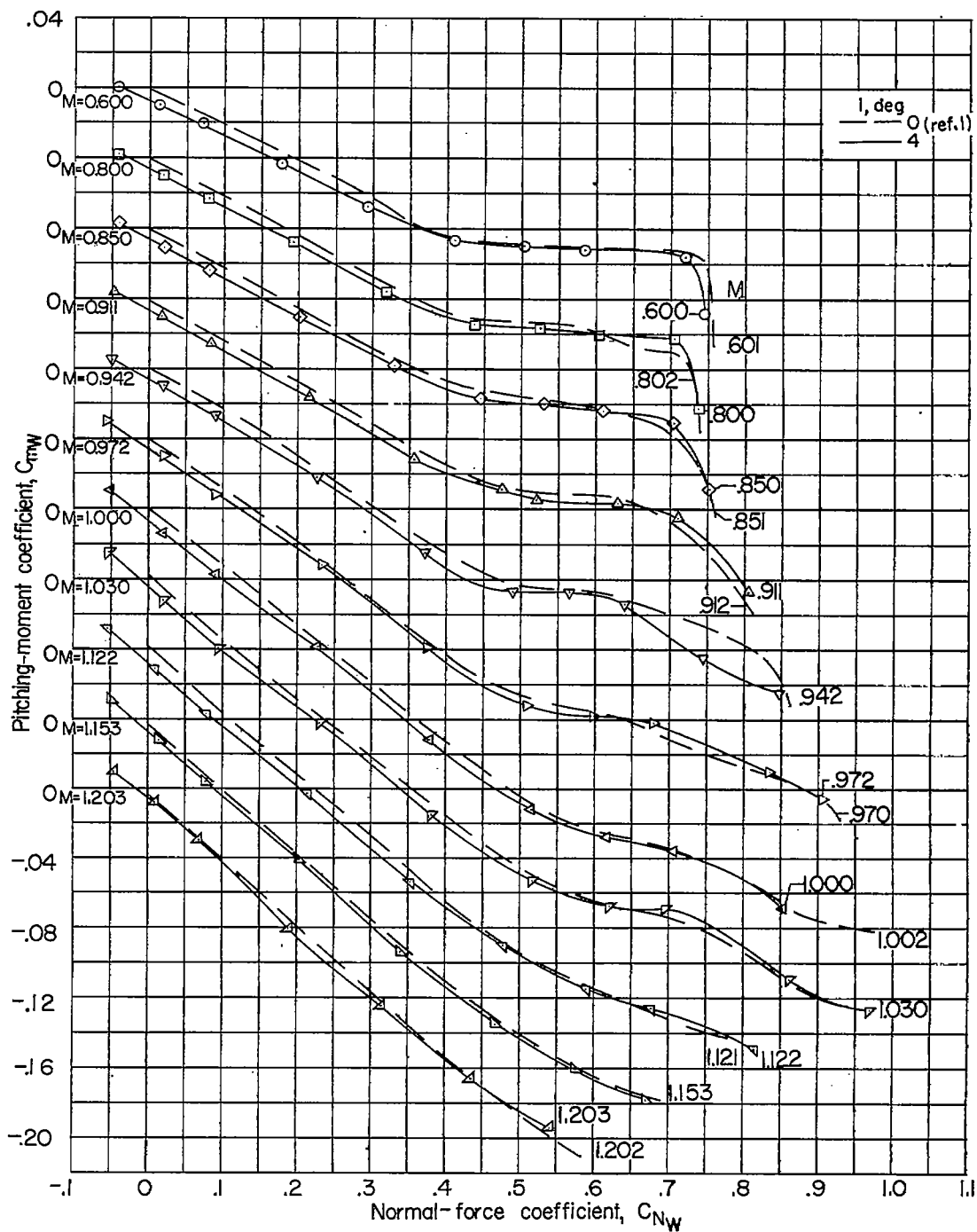
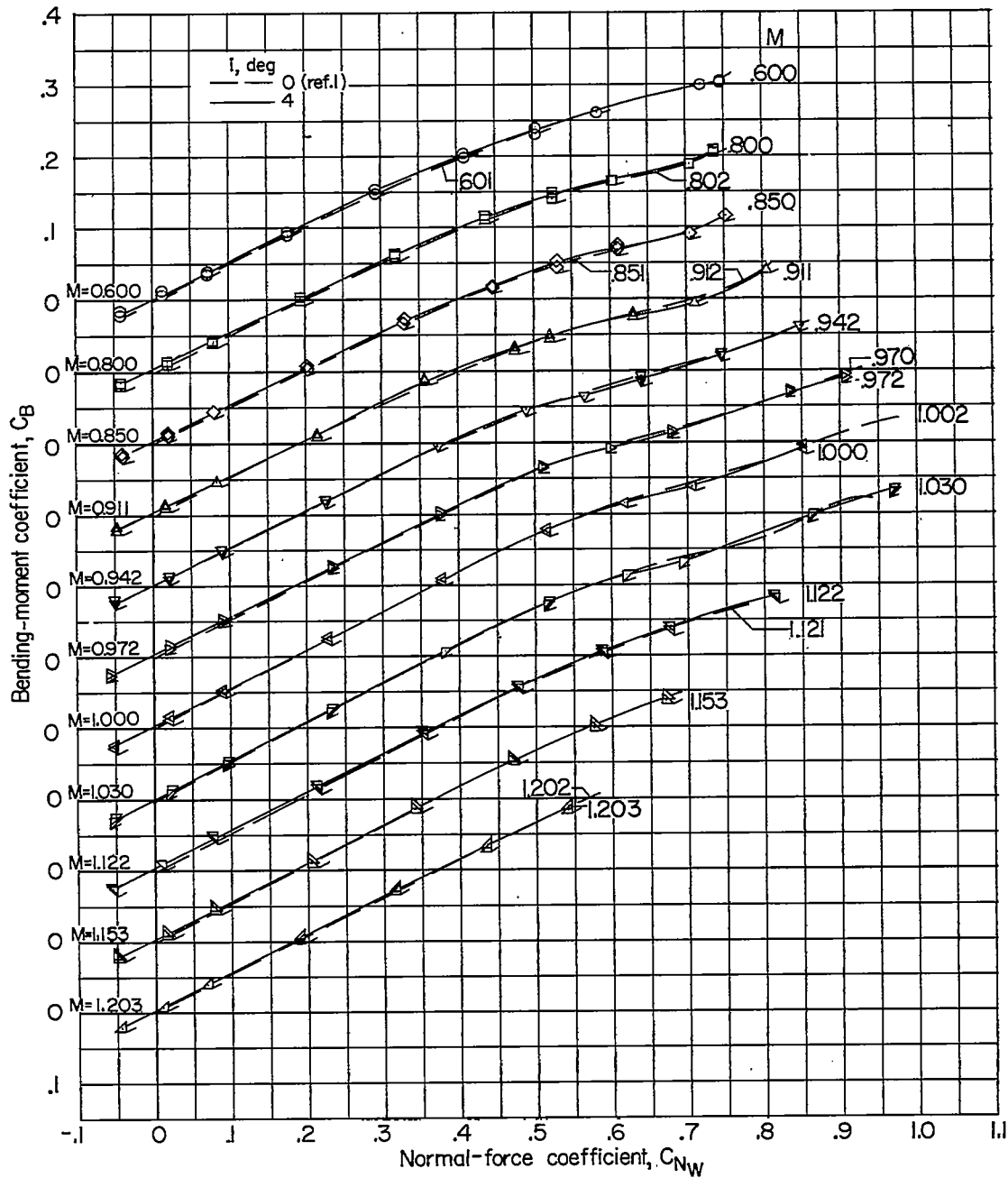
(b) Variation of  $C_{mW}$  with  $C_{Nw}$ .

Figure 8.- Continued.





(c) Variation of  $C_B$  with  $C_{N_W}$  for right- and left-wing panels. Flagged symbols indicate left-wing panel.

Figure 8.- Concluded.

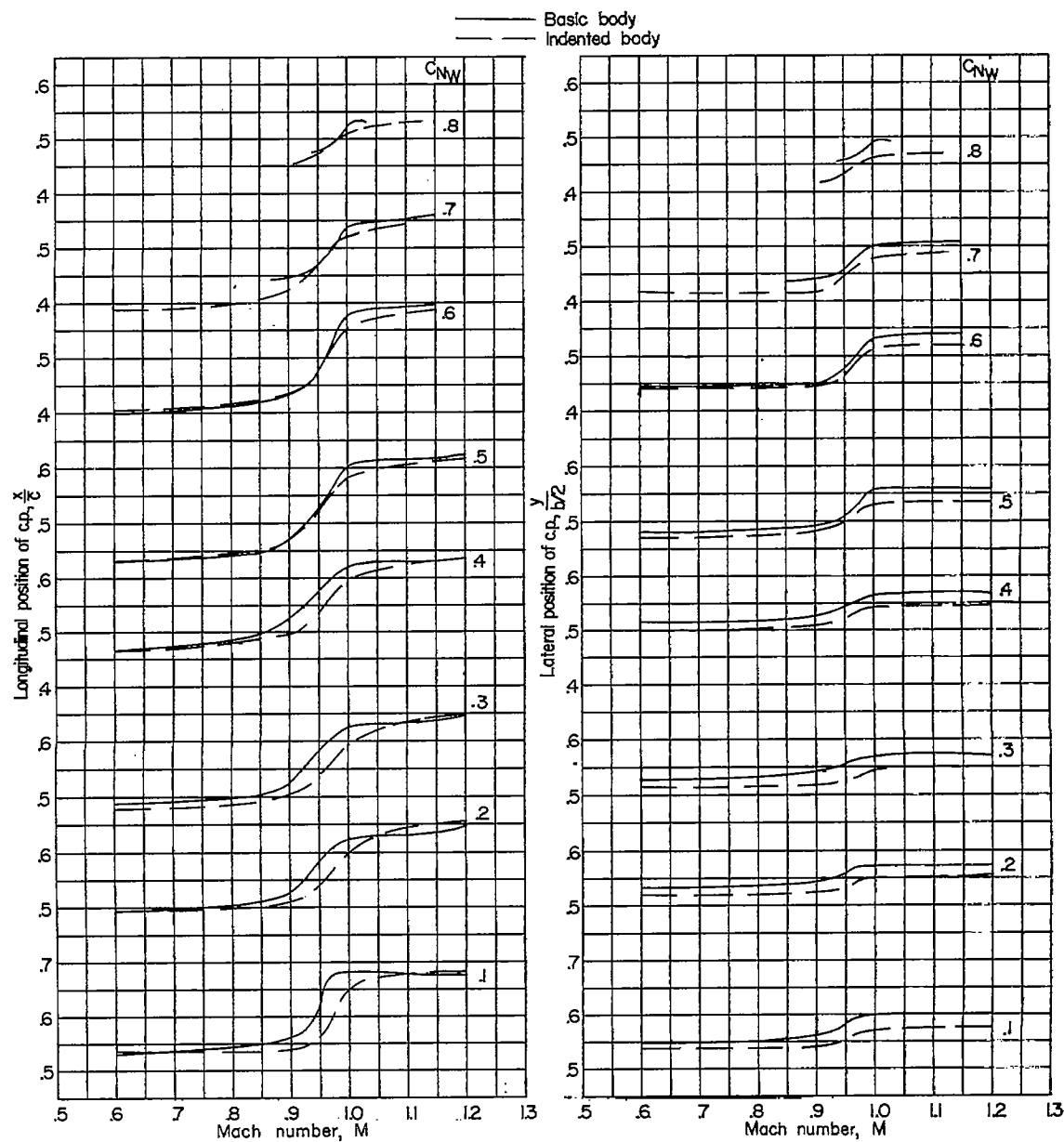


Figure 9.- Effect of body indentation on the variation of the longitudinal and lateral location of the center of pressure with Mach number. Wing incidence  $4^\circ$ .